DEVELOPMENT OF TSUNAMI FORECAST MODEL FOR PORT ORFORD, OREGON

Dylan Righi

August 2009,2009

DRAFT

Contents

Abstract....6
1.0 Background and Objectives....6
2.0 Forecast Methodology....7
2.1 Study Area – context....7
2.2 Tide Gauge data....7
2.3 Historical events....8
2.4 Bathymetry and Topography....8
2.5 Model Setup....9
3.0 Results....9
3.1 Model Validation....9
3.2 Model stability and reliability....10
4.0 Summary and Conclusions....10
5.0 Acknowledgments....11
6.0 References....11
7.0 Appendix A....11
7.1 RIM *.infile for Port Orford, Oregon....11
7.2 SIM *.infile for Port Orford, Oregon....12

DRAFT

List of Tables

Table 1 NGDC run up observations for Port Orford 14

Table 2 MOST Model set up parameters for Port Orford, Oregon..... 15

Table 3 Tsunami sources of 11 historical events used for model validation in this study. 16

Table 4. Unit source combinations used for the 16 artificial mega-events..... 18

DRAFT

List of Figures

Figure 1 Evacuation map for Port Orford, Oregon developed by the Oregon Department of Geology and Mineral Industries in consultation with local officials. It is intended to represent a worst-case scenario for a tsunami caused by an undersea earthquake near the Oregon coast. Evacuation routes were developed by local officials and reviewed by the Oregon Department of Emergency Management. 19

Figure 2 Google Maps image of Port Orford. The yellow arrow indicates the approximate location of the Port Orford tide gauge. 20

Figure 3 Bathemetry (in meters) for the Port Orford RIM grids. The A grid is shown in the top left axis, the B grid in the bottom left, and the C grid on the right. The land topography of the C grid is shown using contours with 25 meter intervals. The red boxes in the A and B plots show the position of the B and C grids, respectively. 21

Figure 4 Bathemetry (in meters) for the Port Orford RIM grids. The A grid is shown in the top left axis, the B grid in the bottom left, and the C grid on the right. The land topography of the C grid is shown using contours with 25 meter intervals. The red boxes in the A and B plots show the position of the B and C grids, respectively. 22

Figure 5 Model results for the 1946 Unimak event. Top left and right axes show, respectively, the SIM and RIM maximum wave height results. The lower axis shows the model wave heights at the geographical position of the Port Orford tide gauge. 23

Figure 6 Model results for the 1994 Kuril event. Top left and right axes show, respectively, the SIM and RIM maximum wave height results. The lower axis shows the model and data wave heights at the Port Orford tide gauge. 24

Figure 7 Model results for the 1996 Andreanof event. Top left and right axes show, respectively, the SIM and RIM maximum wave height results. The lower axis shows the model and data wave heights at the Port Orford tide gauge. 25

Figure 8 Model results for the 2001 Peru event. Top left and right axes show, respectively, the SIM and RIM maximum wave height results. The lower axis shows the model wave heights at the geographical position of the Port Orford tide gauge. 26

Figure 9 Model results for the 2003 Rat Island event. Top left and right axes show, respectively, the SIM and RIM maximum wave height results. The lower axis shows the model wave heights at the geographical position of the Port Orford tide gauge. 27

DRAFT

Figure 10 Model results for the 2006 Tonga event. Top left and right axes show, respectively, the SIM and RIM maximum wave height results. The lower axis shows the model wave heights at the geographical position of the Port Orford tide gauge. 28

Figure 11 Model results for the 2006 Kuril event. Top left and right axes show, respectively, the SIM and RIM maximum wave height results. The lower axis shows the model and data wave heights at the Port Orford tide gauge. 29

Figure 12 Model results for the 2007 Kuril event. Top left and right axes show, respectively, the SIM and RIM maximum wave height results. The lower axis shows the model wave heights at the geographical position of the Port Orford tide gauge. 30

Figure 13 Model results for the 2007 Solomon Islands event. Top left and right axes show, respectively, the SIM and RIM maximum wave height results. The lower axis shows the model wave heights at the geographical position of the Port Orford tide gauge. 31

Figure 14 Model results for the 2007 Peru event. Top left and right axes show, respectively, the SIM and RIM maximum wave height results. The lower axis shows the model wave heights at the geographical position of the Port Orford tide gauge. 32

Figure 15 Model results for the 2007 Chile event. Top left and right axes show, respectively, the SIM and RIM maximum wave height results. The lower axis shows the model wave heights at the geographical position of the Port Orford tide gauge. 33

Figure 16 Wave heights (in meters) from the SIM model at the location of the Port Orford tide gauge for 16 hypothetical mega-tsunami scenarios. The x-axis units are hours since the event earthquake. 34

DRAFT

Development of a Tsunami Forecast Model for Port Orford, Oregon

Dylan Righi

DRAFT

Abstract

The Short-term Inundation Forecasting for Tsunamis (SIFT) system is under development by the NOAA Center for Tsunami Research (NCTR) at the Pacific Marine Environmental Laboratory (PMEL) to provide Tsunami Warning Centers (TWCs) with a capability to produce efficient forecasts for tsunami arrival time, heights and inundation for the target coastlines given a tsunami event. The development of Standby Inundation Model for Port Orford, Oregon is described as a component of the SIFT system. The optimized SIM can provide a 4-hour local forecast of first wave arrival, amplitudes and reasonable inundation limit in minutes. It shows robust results for all historical validation and stability test cases.

1.0 Background and Objectives

An efficient tsunami forecast system provides timely basin-wide warning of in-progress tsunami waves accurately and quickly (Titov et al., 2005). NOAA's Short-term Inundation Forecast of Tsunami (SIFT) is an advanced tsunami forecasting system that combines real-time tsunami event data with numerical models to produce estimates of tsunami wave arrival times and amplitudes. The SIFT system integrates several key components: the tsunameters for real-time monitoring of tsunami signals in the deep ocean, a basin-wide pre-computed propagation database of water level and flow velocities based on potential seismic unit sources, an inversion algorithm to derive the tsunami source based on the tsunameter observations during a tsunami event, and the Stand-by Inundation Models (SIMs) to provide accurate and speedy numerical modeling of tsunami impact for coastal communities. A SIM is used to create the forecast model to provide an estimate of wave arrival time, wave height, and inundation immediately after a tsunami event. Tsunami forecast models are run in real time while a tsunami is propagating in the open ocean; consequently they are designed to perform under very stringent time limitations. The Stand-by Inundation Model (SIM), based on the Method of Splitting Tsunami (MOST), emerges as the solution in SIFT by modeling real-time tsunami in minutes while employing high resolution grids. Each SIM consists of three telescoped grids with increasing spatial resolution, and temporal resolution for simulation of wave inundation onto dry land.

The SIM utilizes the most recent bathymetry and topography available to reproduce the correct wave dynamics during the inundation computation. SIMs are constructed for populous coastal communities at risk for tsunamis in the Pacific, Atlantic and Caribbean. Previous and present development of SIM in the Pacific (Titov et al., 2005; Titov, 2009; Tang et al., 2008; Wei et al., 2008) has shown the accuracy and efficiency of the up-to-date SIMs implemented in SIFT in the real-time tsunami forecast, as well as in hindcast research.

The objective of SIM development is to provide real-time tsunami predictions for selected coastal locations while the tsunami is propagating through the open ocean, before the waves have reached many coastlines. SIMs will be incorporated into the U.S. tsunami warning system for use at the Pacific and West Coast-Alaska Tsunami Warning Center. Titov and Gonzalez (1997) and Tang et al (2008) describe the technical aspects of SIM development, stability testing and robustness.

DRAFT

2.0 Forecast Methodology

The methodology for modeling these coastal areas is to develop a set of three nested grids (A, B, C), each of which is successively finer in resolution, until the near-shore details can be resolved to the point that tide gauge data from historical tsunamis in the area match reasonably with the modeled results. The procedure is to start with large spatial extent merged bathymetric topographic grids at high resolution, referred to as a "reference SIM" (RIM), and then after a reasonable data fit is achieved to optimize these grids by coarsening the resolution and shrinking the grid size until the model runs in under 10 min of wall-clock time. This allows for the significant portion of the modeled tsunami waves, typically 4 to 10 hr of modeled tsunami time, to pass through the model domain without too much signal degradation. This final model is referred to as the "optimized SIM".

2.1 Study Area – context

Port Orford is located inshore of Port Orford Head, a rocky coastal head with elevations greater than 200 feet. To the north of the Head the beach is wide and flat. Garrison Lake is a shallow coastal lake, separated from the ocean by a sand dune spit, and a number of houses are built close to the lake. To the south of Port Orford Head is a wide southwestern facing bay that is bounded by Humbug Mountain to the south. The bay contains a number of sea stacks which, as we will see, are significant for the modeling effort. Lastly of interest, just to the north on the coast is Cape Blanco, the westernmost point of the contiguous United States.

Port Orford is located on the southwestern Oregon coast, between the larger communities of Bandon to the north and Gold Beach to the south. According to the 2000 U.S. census, Port Orford had a population of 1153. Economically, the community currently relies on commercial fishing and tourism, with logging playing a smaller but still viable part. Since Port Orford is not situated on a protected riverine harbor, and the bay is open to input from ocean storm energy, the fishing fleet depends on a dry dock system. Called a "dolly dock" because boats are lifted out of the water by one of two cranes and placed on dollies, the dock recently underwent a $5.5 million refurbishment and houses 60 commercial vessels and is host to area sports fishermen. Port Orford is located on US Highway 101, the "Oregon Coast Highway", and like many Oregon coastal communities, is dependent on it for transport and possible evacuations.

The evacuation map for Port Orford developed by the Oregon Department of Geology and Mineral Industries is shown in Fig 1. To the south of Port Orford Head the vulnerable zones are mostly limited to undeveloped areas near the shoreline, with the exception of the lower elevation area near Highway 101. The other notable exception is the Port Orford dock, located inside of Graveyard Point. To the north of Port Orford the evacuation zone is larger, owing to the lower elevations and the presence of Garrison Lake. There are a number of residences in this area that could be threatened by a high-energy tsunami event.

2.2 Tide Gauge data

Data from the Port Orford tide gauge was used to verify the model results presented in this report. The tide gauge is located on the end of the of the Port Orford dock at N 42.738972, W 124.498278. The tide gauge instrument shack can be see in Fig (XXX dock photo XXX) at the southern (left) corner of the dock. Also, the yellow arrow in Fig. 2 points to the approximate location of the tide gauge. The mean high water is XXX Mean sea level is XXX Mean range is XXXX.

DRAFT

Before being used to compare with and validate the modeled water level time series, the tide gauge data is de-tided and smoothed. First, to eliminate obvious outlier data points, a running-mean filter with a width of one hour is used to construct a smoothed time series. Then any point in the original time series whose difference from the running mean is greater than 6 times the standard deviation of the difference is discarded. The tidal signal and instrument noise were removed using a band-pass Fourier filter with cut-offs of 8 minutes and 3 hours. The resulting time series are seen in Figures 7, 8, 9, 10, 12 and 13.

2.3 Historical events

Historical data of run-up as a result of tsunamis is available for three events and were used for model verification – 1994 Kuril, 1996 Andreanov and 2006 Kuril. NGDC tsunami run up database returns fourteen events where run up was noted in Port Orford (http://www.ngdc.noaa.gov/hazard/tsu_db.shtml, last accessed September 29,2009). These events are listed in Table 1.

2.4 Bathymetry and Topography

Accurate bathymetry and topography are crucial inputs to developing the reference and standby models, especially for the inundation of the near-shore environment. To develop each grid, we attempt to gather and use the best available data for the area studied. Grids may be updated if newer, more accurate data are available. For the development of the Port Orford grids, a 1/3-arc-sec merged bathymetric and topographic digital elevation model was developed by NGDC for tsunami inundation modeling. To increase the size of the grids to encompass the larger B grid and the regional A grid, a 6-sec Oregon coast grid and a 36-sec Pacific Northwest grid were combined, resampled, and error checked to extend the domain for the grid extents. Grids are made available in the ESRI ArcGIS raster format. Additionally, all data were converted to the WGS 84 vertical datum.

Final grids used for the reference and standby models are described in Table 2 and Figs. 3 and 4. Each set of grids is nested with increasing resolution from the larger regional grids to the higher resolution community-based grid. The RIM A grid extent is region wide, covering from central Washington on the northern boundary and south to almost San Francisco Bay in central California at a 36 arc second resolution. The A grid depth reached a maximum of 5400 m. The B grid has a resolution of 6 arc-seconds and its extent was reduced to cover most of Oregon and part of northern California. The grid was able to extend to an offshore depth of ~1800 m. The Reference C grid extends north to cover the lower lying areas around Garrison Lake and past the Humbug Mountain point in the south. With grid spacing of 1/3 arc-second, or ~10 meters, it is the highest resolution grid used. The maximum depth of the C grid is 92 m. The grid extent was defined to focus the study on the effects of tsunami waves on the occupied areas of Port Orford. The authors decided covering the bay area to the south of Port Orford was important to describe how waves moved up the coast to Port Orford. The Garrison Lake area is also important since there are residences there at lower elevations that could be endangered by high waves.

The SIM grids all keep the same extents as the RIM grid, but their resolution is reduced in order to allow the models to be processed faster. The SIM A, B and C resolutions are 72, 12 and 2 arc-seconds respectively. These resolutions allow a time step of 1 second to be used for the SIM model runs.

DRAFT

Under model testing, it was discovered that the RIM model developed instabilities at three locations during stronger events (for instance, the 1946 Unimak historical event). These manifested themselves as very strong wave-height 'ringing' emanating from singular grid points. The unstable points were around the sea stacks in the bay southeast of Port Orford at ~42 44'N, the sea stacks further south and to the northwest of Humbug Mountain (at ~42° 42"N), and most significantly between the point of Port Orford Head and the elongated sea stack offshore. The bathymetries of all three of these areas were smoothed using a centered five-point smoother. This initial smoothing removed the first two unstable regions, but the Port Orford Head point still exhibited problems. Further smoothing and a reducing the model time-step also failed to remove the instability. Finally, the model friction parameter was increased, allowing the model to run successfully. A sensitivity study was undertaken and a value of 0.003 was found to be optimal, in terms of reducing instabilities and at the same time, keeping the friction parameter near the standard value of 0.0009. Not that this change was only made in the RIM runs, since the SIM model did not have the same instability issues.

2.5 Model Setup

The model used to estimate tsunami amplitude is the MOST model (Titov and González, 1997; Synolakis et al., 2007; Tang et al., 2008), which is a finite difference method of characteristic model which takes input from a propagation-run data base and then, via a series of nested grids, resolves the near-shore bathymetry and topography to estimate the water level at coastal sites. Adjustable parameters include time step, number of time steps, near shore wet/dry boundary depth, coarse grid wet/dry boundary depth, run down or not in coarse grids friction coefficient, output time, grid size, grid resolution, and grid position. Once tested, these parameters remain fixed from run to run, under the assumption that the parameters and features may be location dependent, including sharp bathymetric changes and high-resolution grids needed to resolve for channels, but should not depend on the flow field. For Port Orford the grid resolution and extents for the reference and optimized (stand-by) grids are given in Table 2. Figures of the model extents for reference and optimized grids are shown in Figs. 3 and 4.

DRAFT

3.0 Results

3.1 Model Validation

Several events were used to test the Newport RIM and SIM development. The eleven events used and their time, location and source description are presented in Table 2. In addition, tide gauge data was available for model verification for the following events: 1994 Kuril, 1996 Andreanof, and the 2006 Kuril tsunami events.

Comparisons of the RIM and SIM model results and, when available, the tide gauge data are shown in Figs. 5 - 15 for the historical events. In each figure, the top left and right panels show, respectively, the SIM and RIM maximum wave heights (cms). The bottom panel shows the wave heights at the location of the Port Orford tide gauge as a function of time since the event. Note that the color scale and plot limits change with event.

The 1946 Unimak event is the largest historical event modeled for this this report. The maximum height patterns at Port Orford (Fig. 5) predicted by the SIM and RIM models compare well. The SIM predicts higher waves in the bay, while the RIM is higher in the Garrison Lake coastal area. The wave height time series at the tide gauge shows that the SIM matches well with the higher resolution RIM. The initial waves are the same and it's not until

past the fifth or sixth wave peak that there is any significant differences between the predictions.

The 1994 Kuril earthquake, showed very good agreement between SIM and RIM maximum wave heights predicted. Also encouraging is the comparison of the tide gauge time series: the predicted SIM and RIM wave heights do very well at tracking the tide gauge data. The initial wave is well represented and is followed by subsequent higher peaks. The tide gauge does show higher peaks around the 11 hours after the event, and the models do over-predict the 12 hour peak, but the general correlations are good.

The 1996 Andreanof event resulted in smaller maximum wave heights - less than 10 centimeters in the Port Orford RIM and SIM predictions. The lower energy of the tsunami response makes the comparison between time series and predictions less clear due to the noise in the data. Bet there are some similarities: the initial wave at ~5.5 hours and the peaks around 6.5 seem to reflect values seen in the data (Fig. 7).

Results from the 2006 Kuril event showed waves consistently higher than the RIM/SIM predictions. The arrival of the first wave in the predictions is reflected in the data, but after that it's hard to find consistent correlation between individual peaks. The reason for this requires further investigation. But the comparison between the low resolution SIM and the high resolution RIM is good, both in the maximum wave height plots and in the time series (Fig 11).

Simulations of the 2001 Peru (Fig. 8), 2003 Rat Island (Fig. 9), 2006 Tonga (Fig. 10), 2007 Solomon Islands (Fig. 13), 2007 Peru (Fig. 14), and 2007 Chile (Fig. 15), events are all smaller events and don't result in waves over 10 centimeters at Port Orford. The SIM and RIM predictions for all these events compare very well, both in the maximum waves predicted and in the timing and magnitude of the waves at the tide gauge location.

3.2 Model stability and reliability

Recorded historical tsunamis provide only a limited number of events, from limited locations. More comprehensive test cases of destructive tsunamis with different directionalities are needed to check the stability and robustness for SIMs. To this end, a subset of 16 synthetic T_{Mw} 9.3 tsunamis as in Tang *et al.* (2008) was selected for further examination. The sources used as input to the computational grids are from the propagation database developed by NCTR (Gica *et al.*, 2008). Table 4 lists the 16 synthetic tsunami events used here and their unit source combinations.

The resulting modeled wave height signals at the tide gauge location from the developed SIM are shown in Fig 16. The most severe wave height signal is caused by the S06_acsz scenario, a Mwt 9.3 event on the nearby Cascadian subduction fault. Wave heights reach 8 meters for this event. The S18_kisz scenario causes the second largest simulated waves seen at Port Orford, from an earthquake on the other side of the Pacific on the Kamchatka-Yap section. In contrast, mega-events that occur in Central and South America and the South Pacific result in smaller wave heights for Port Orford. Those, while still significant, are not as dramatic. Lastly, note that the SIM developed for Port Orford is numerically stable for all these mega-events, and can withstand the very high energies released.

4.0 Summary and Conclusions

We have developed reference and forecast models for Port Orford, Oregon.
The computational grids were derived from the best available bathymetric and

DRAFT

topographic source data available. Testing and comparison was undertaken using eleven historical tsunami events. The SIMS were validated by comparing predicted wave heights and velocities with a higher resolution RIM model, and with data available from the Port Orford tide gauge.

In addition, the stability and sensitivity of the model were tested with 16 Mw 9.3 synthetic tsunami scenarios originating around the Pacific Rim and South American coast. The forecast model remained stable during the synthetic testing. Scenarios run using Alaska-Cascadia and Kuril-Kamchatka sources would result in waves as high as 8 m. The forecast model can provide a 4-hr forecast model of the first wave arrival, amplitudes, and inundation within 10 min of clock time.

5.0 Acknowledgments

I would like to thank Nazila Merati for editorial assistance in the writing of this report and Yong Wei for his assistance with model setup and troubleshooting. This publication is partially funded by the Joint Institute for the Study of the Atmosphere and Ocean (JISAO) under NOAA Cooperative Agreement No. NA17RJ1232, JISAO Contribution No. xxxx. This is PMEL Contribution No. XXXX.

6.0 References

Forthcoming

7.0 Appendix A

7.1 RIM *.infile for Port Orford, Oregon

```
0.001 Minimum amplitude of input offshore wave (m):
5     Input minimum depth for offshore (m)
0.1   Input "dry land" depth for inundation (m)
0.003     Input friction coefficient (n**2)
1       let a and b run up
100.0    max eta before blow up (m)
.125  Input time step (sec)
230400      Input amount of steps
12    Compute "A" arrays every n-th time step, n=
4     Compute "B" arrays every n-th time step, n=
360   Input number of steps between snapshots
0     ...Starting from
1     ...Saving grid every n-th node, n=
portorfordA_1.most
```

DRAFT

7.2 SIM *.infile for Port Orford, Oregon

```
0.0001      Minimum amplitude of input offshore wave (m):
5     Input minimum depth for offshore (m)
0.1   Input "dry land" depth for inundation (m)
0.0009     Input friction coefficient (n**2)
1       let a and b run up
100.0    max eta before blow up (m)
1.    Input time step (sec)
36000 Input amount of steps
5     Compute "A" arrays every n-th time step, n=
2     Compute "B" arrays every n-th time step, n=
90    Input number of steps between snapshots
0     ...Starting from
1     ...Saving grid every n-th node, n=
```

DRAFT

DRAFT

Table 1 NGDC run up observations for Port Orford

DRAFT

		Reference Inundation Model(RIM)			Stand by Inundation Model (SIM)		
Grid	**Region**	**Coverage Lat (W) Long (N)**	**Cell size**	**Time Step [sec]**	**Coverage Long (W) Lat (N)**	**Cell Size**	**Time Step [sec]**
A	Central Oregon and South West Washington	39.0 – 47.19 124.5 – 123.51	36		39.01 – 47.19 127.5 – 123.5	72	
B	Oregon Coast	42.0667 - 43.265 124.933 - 124.2683	6		42.0683 - 43.265 124.933 - 124.27	12	
C	Port Orford	42.6714 – 42.7732 124.5510 – 124.4306	0.33	0.125	42.6715 – 42.7732 124.5510 – 124.4304	2	1.0
Minimum offshore depth (m)		5			5		
Water depth for dry land (m)		0.1			0.1		
Manning coefficient, n		0.003			0.0009		
CPU time needed for a 4 hour simulation		25 hr			13.4 min		

Table 2 MOST Model set up parameters for Port Orford, Oregon

DRAFT

Event	Time (UTC)	Zone	Mw	Lon	Lat	Source
Chile	2007.11.14 15:40:52	SASZ	7.6	69.9W	22.2S	0.81×a22 + 0.33×a23 + 0.11×b23
Peru	2007.08.15 23:40:57	SASZ	8.1	76.509W	13.354S	4.3×a9 + 4.1×b9
Solomon	2007.04.01 20:40:40.7	NBSV	8.2	156.4E	7.96S	12.0×b10
Kuril	2007.01.13 04:23:48.2	KISZ	7.9	154.80E	46.18N	-3.82×b13
Kuril	2006.11.15 11:14:16	KISZ	8.1	154.32E	46.75N	4.0×a12 + 0.5×b12 + 2.0×a13 + 1.5×b13
Tonga	2006.05.03 15:26:39	NZKT	8.1	174.164W	20.13N	8.44×b29
Rat Island	2003.11.17 06:43:07	AASZ	7.8	178.74E	51.13N	2.81×b11
Peru	2001.06.23 20:33:14	SASZ	8.2	73.31W	16.14S	5.7×a15 + 2.9×b16 + 1.98×a16
Andreanof	1996.06.10 04:03:35.4	AASZ	7.8	176.847E	51.478N	2.4×a15 + 0.8×b16
Kuril	1994.10.04 13:22:58.3	KISZ	8.1	147.328E	43.706N	9.0×a20
Unimak	1946.04.01 12:28:56	AASZ	8.1	163.19W	53.32	7.5×b23 + 19.70×b24 + 3.7×b25

Table 3 Tsunami sources of 11 historical events used for model validation in this study.

DRAFT

Event	Source
S01_kisz_ab22T31	Kamchatka-Yap, Pacific grid: Mwt 9.3, 29.00*a22+29.00*b22+29.00*a23+29.00*b23+29.00*a24+29.00*b24+29.00*a25+29.00*b25+29.00*a26+29.00*b26+29.00*a27+29.00*b27+29.00*a28+29.00*b28+29.00*a29+29.00*b29+29.00*a30+29.00*b30+29.00*a31+29.00*b31
S02_kisz_ab1T10	Kamchatka-Yap, Pacific grid: Mwt 9.3, 29.00*a1+29.00*b1+29.00*a2+29.00*b2+29.00*a3+29.00*b3+29.00*a4+29.00*b4+29.00*a5+29.00*b5+29.00*a6+29.00*b6+29.00*a7+29.00*b7+29.00*a8+29.00*b8+29.00*a9+29.00*b9+29.00*a10+29.00*b10
S03_acsz_ab12T21	Aleutian-Cascadia, Pacific grid: Mwt 9.3, 29.00*a12+29.00*b12+29.00*a13+29.00*b13+29.00*a14+29.00*b14+29.00*a15+29.00*b15+29.00*a16+29.00*b16+29.00*a17+29.00*b17+29.00*a18+29.00*b18+29.00*a19+29.00*b19+29.00*a20+29.00*b20+29.00*a21+29.00*b21
S04_acsz_ab22T31	Aleutian-Cascadia, Pacific grid: Mwt 9.3, 29.00*a22+29.00*b22+29.00*a23+29.00*b23+29.00*a24+29.00*b24+29.00*a25+29.00*b25+29.00*a26+29.00*b26+29.00*a27+29.00*b27+29.00*a28+29.00*b28+29.00*a29+29.00*b29+29.00*a30+29.00*b30+29.00*a31+29.00*b31
S05_acsz_ab38T47	Aleutian-Cascadia, Pacific grid: Mwt 9.3, 29.00*a38+29.00*b38+29.00*a39+29.00*b39+29.00*a40+29.00*b40+29.00*a41+29.00*b41+29.00*a42+29.00*b42+29.00*a43+29.00*b43+29.00*a44+29.00*b44+29.00*a45+29.00*b45+29.00*a46+29.00*b46+29.00*a47+29.00*b47
S06_acsz_ab56T65	Aleutian-Cascadia, Pacific grid: Mwt 9.3, 29.00*a56+29.00*b56+29.00*a57+29.00*b57+29.00*a58+29.00*b58+29.00*a59+29.00*b59+29.00*a60+29.00*b60+29.00*a61+29.00*b61+29.00*a62+29.00*b62+29.00*a63+29.00*b63+29.00*a64+29.00*b64+29.00*a65+29.00*b65
S07_sasz_ab1T10	Central America, Pacific grid: Mwt 9.3, 29.00*a1+29.00*b1+29.00*a2+29.00*b2+29.00*a3+29.00*b3+29.00*a4+29.00*b4+29.00*a5+29.00*b5+29.00*a6+29.00*b6+29.00*a7+29.00*b7+29.00*a8+29.00*b8+29.00*a9+29.00*b9+29.00*a10+29.00*b10
S09_sasz_ab40T49	South American, Pacific grid: Mwt 9.3, 29.00*a40+29.00*b40+29.00*a41+29.00*b41+29.00*a42+29.00*b42+29.00*a43+29.00*b43+29.00*a44+29.00*b44+29.00*a45+29.00*b45+29.00*a46+29.00*b46+29.00*a47+29.00*b47+29.00*a48+29.00*b48+29.00*a49+29.00*b49
S11_ntsz_ab20T29	New Zealand-Kermadec-Tonga, Pacific grid: Mwt 9.3, 29.00*a20+29.00*b20+29.00*a21+29.00*b21+29.00*a22+29.00*b22+29.00*a23+29.00*b23+29.00*a24+29.00*b24+29.00*a25+29.00*b25+29.00*a26+29.00*b26+29.00*a27+29.00*b27+29.00*a28+29.00*b28+29.00*a29+29.00*b29
S12_ntsz_ab30T39	New Zealand-Kermadec-Tonga, Pacific grid: Mwt 9.3, 29.00*a30+29.00*b30+29.00*a31+29.00*b31+29.00*a32+29.00*b32+29.00*a33+29.00*b33+29.00*a34+29.00*b34+29.00*a35+29.00*b35+29.00*a36+29.00*b36+29.00*a37+29.00*b37+29.00*a38+29.00*b38+29.00*a39+29.00*b39

DRAFT

S13_nvsz_ab28T37	New Britain-Solomons-Vanuatu, Pacific grid: Mwt 9.3, 29.00*a28+29.00*b28+29.00*a29+29.00*b29+29.00*a30+29.00*b30+29.00*a31+29.00*b31+29.00*a32+29.00*b32+29.00*a33+29.00*b33+29.00*a34+29.00*b34+29.00*a35+29.00*b35+29.00*a36+29.00*b36+29.00*a37+29.00*b37
S14_mosz_ab1T10	Manus OCB, Pacific grid: Mwt 9.3, 29.00*a1+29.00*b1+29.00*a2+29.00*b2+29.00*a3+29.00*b3+29.00*a4+29.00*b4+29.00*a5+29.00*b5+29.00*a6+29.00*b6+29.00*a7+29.00*b7+29.00*a8+29.00*b8+29.00*a9+29.00*b9+29.00*a10+29.00*b10
S15_ngsz_ab3T12	North New Guinea, Pacific grid: Mwt 9.3, 29.00*a3+29.00*b3+29.00*a4+29.00*b4+29.00*a5+29.00*b5+29.00*a6+29.00*b6+29.00*a7+29.00*b7+29.00*a8+29.00*b8+29.00*a9+29.00*b9+29.00*a10+29.00*b10+29.00*a11+29.00*b11+29.00*a12+29.00*b12
S16_epsz_ab6T15	East Philippines, Pacific grid: Mwt 9.3, 29.00*a6+29.00*b6+29.00*a7+29.00*b7+29.00*a8+29.00*b8+29.00*a9+29.00*b9+29.00*a10+29.00*b10+29.00*a11+29.00*b11+29.00*a12+29.00*b12+29.00*a13+29.00*b13+29.00*a14+29.00*b14+29.00*a15+29.00*b15
S17_rnsz_ab12T21	Ryukus-Kyushu-Nankai, Pacific grid: Mwt 9.3, 29.00*a12+29.00*b12+29.00*a13+29.00*b13+29.00*a14+29.00*b14+29.00*a15+29.00*b15+29.00*a16+29.00*b16+29.00*a17+29.00*b17+29.00*a18+29.00*b18+29.00*a19+29.00*b19+29.00*a20+29.00*b20+29.00*a21+29.00*b21
S18_kisz_ab32T41	Kamchatka-Yap, Pacific grid: Mwt 9.3, 29.00*a32+29.00*b32+29.00*a33+29.00*b33+29.00*a34+29.00*b34+29.00*a35+29.00*b35+29.00*a36+29.00*b36+29.00*a37+29.00*b37+29.00*a38+29.00*b38+29.00*a39+29.00*b39+29.00*a40+29.00*b40+29.00*a41+29.00*b41

Table 4. Unit source combinations used for the 16 artificial mega-events.

DRAFT

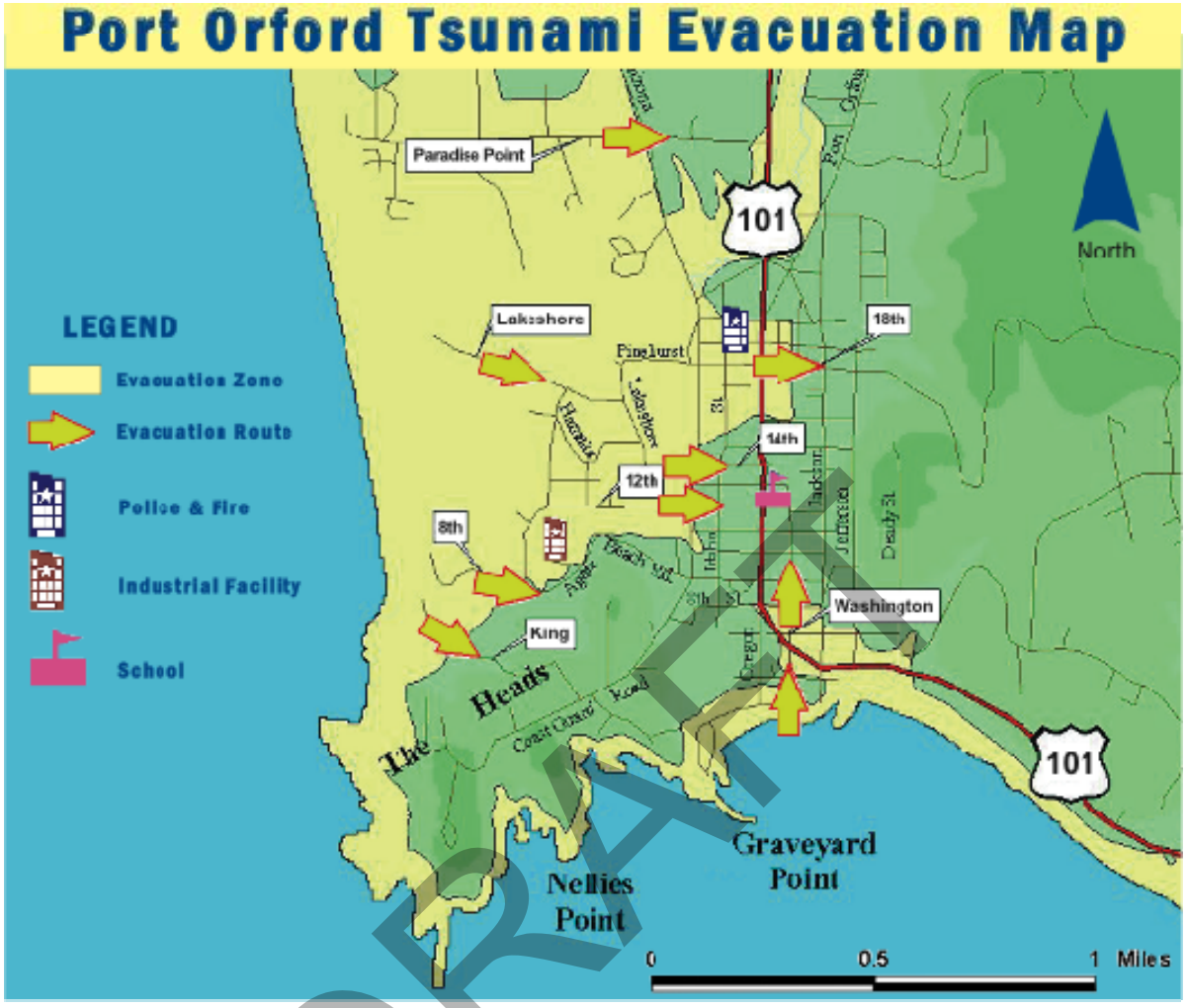

Figure 1 Evacuation map for Port Orford, Oregon developed by the Oregon Department of Geology and Mineral Industries in consultation with local officials. It is intended to represent a worst-case scenario for a tsunami caused by an undersea earthquake near the Oregon coast. Evacuation routes were developed by local officials and reviewed by the Oregon Department of Emergency Management.

DRAFT

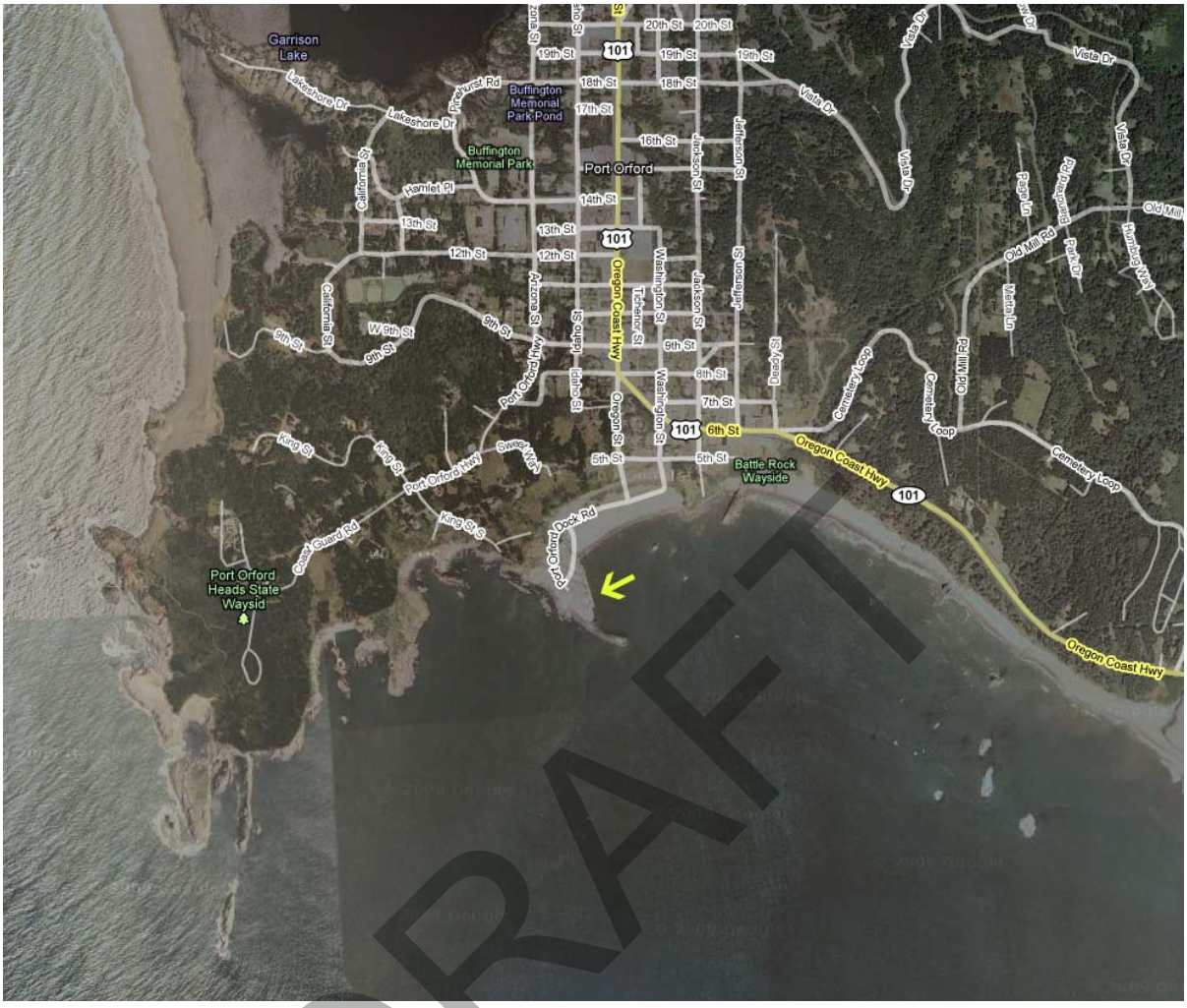

Figure 2 Google Maps image of Port Orford. The yellow arrow indicates the approximate location of the Port Orford tide gauge.

DRAFT

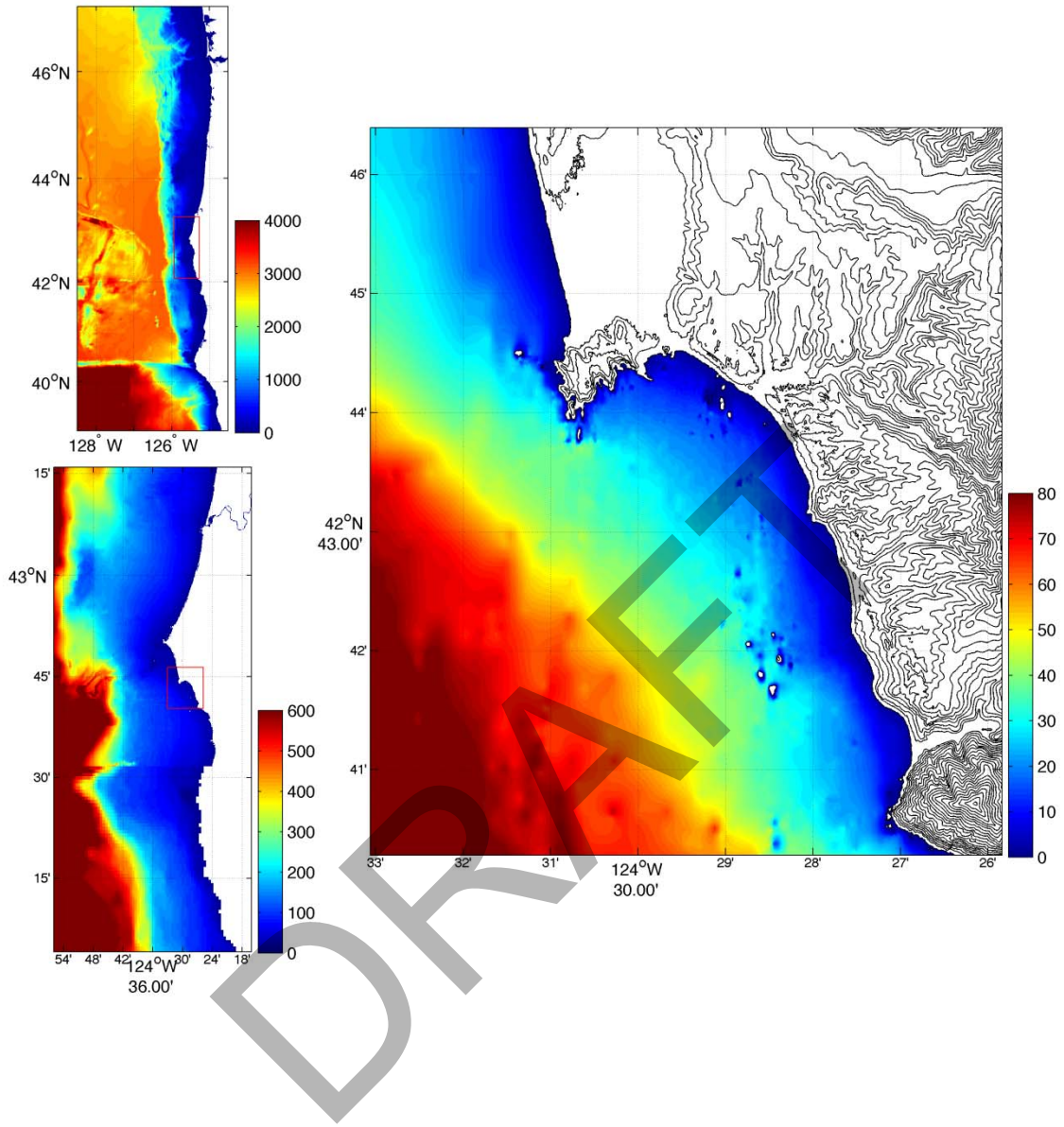

DRAFT

Figure 3 Bathemetry (in meters) for the Port Orford RIM grids. The A grid is shown in the top left axis, the B grid in the bottom left, and the C grid on the right. The land topography of the C grid is shown using contours with 25 meter intervals. The red boxes in the A and B plots show the position of the B and C grids, respectively.

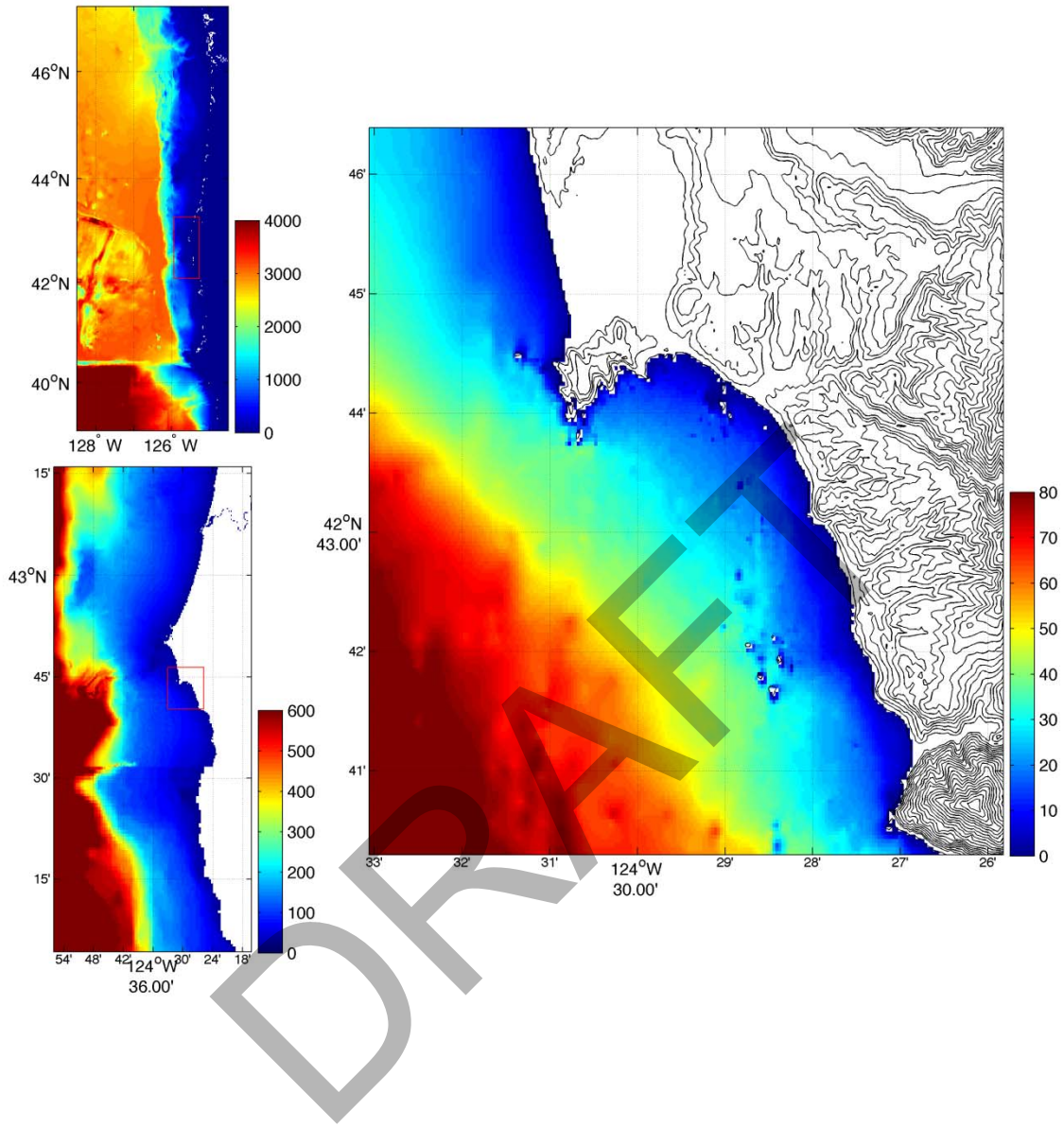

DRAFT

Figure 4 Bathemetry (in meters) for the Port Orford RIM grids. The A grid is shown in the top left axis, the B grid in the bottom left, and the C grid on the right. The land topography of the C grid is shown using contours with 25 meter intervals. The red boxes in the A and B plots show the position of the B and C grids, respectively.

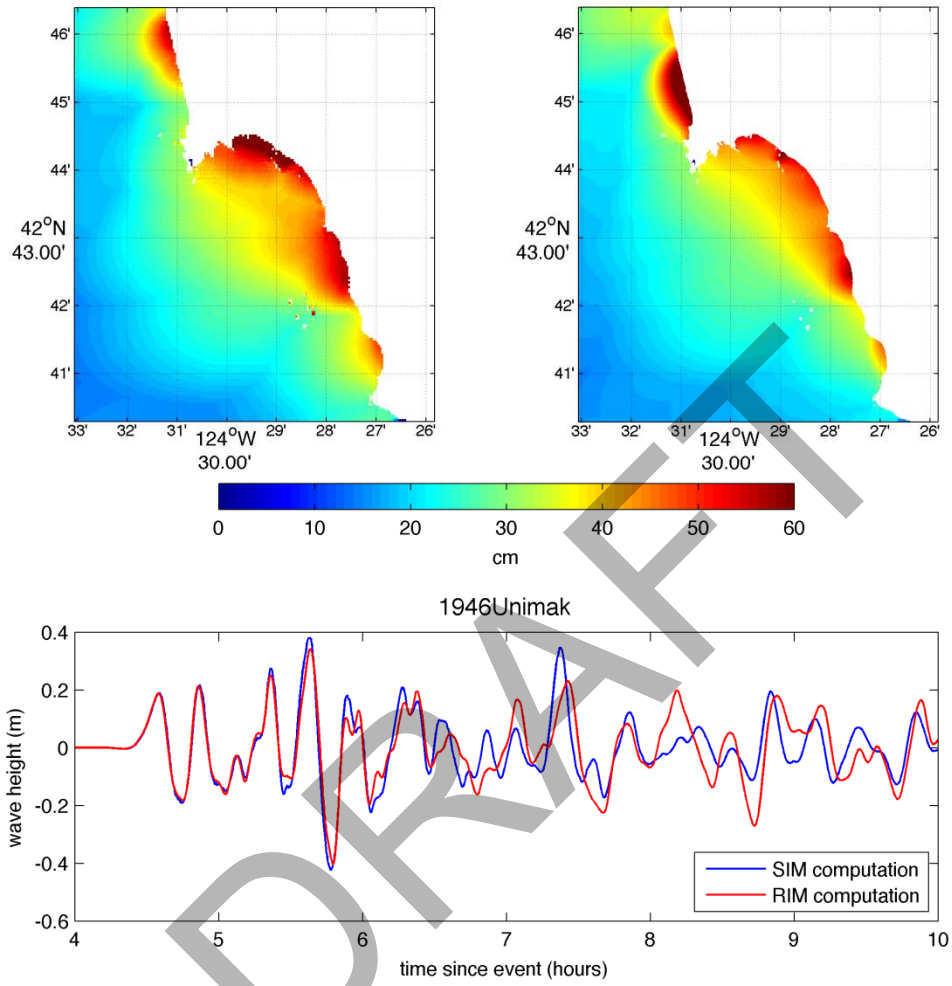

DRAFT

.

Figure 5 Model results for the 1946 Unimak event. Top left and right axes show, respectively, the SIM and RIM maximum wave height results. The lower axis shows the model wave heights at the geographical position of the Port Orford tide gauge.

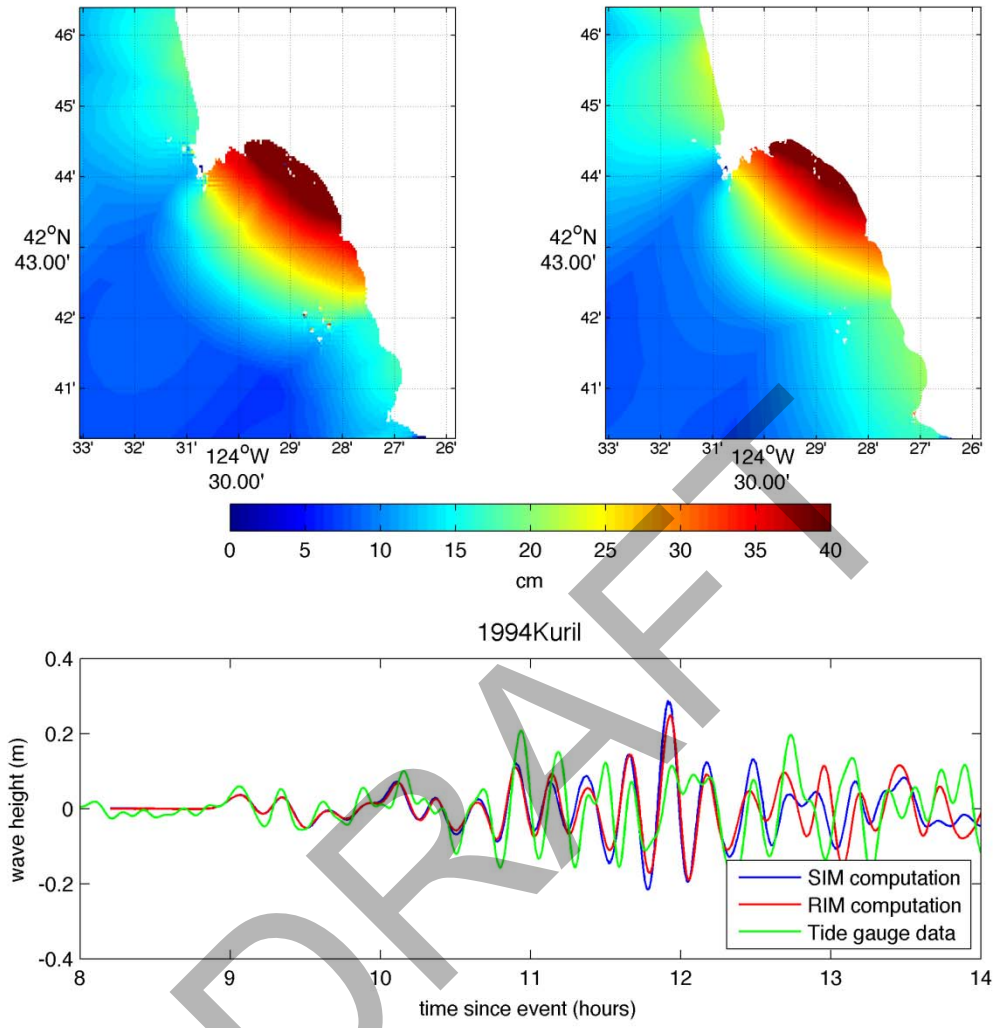

DRAFT

Figure 6 Model results for the 1994 Kuril event. Top left and right axes show, respectively, the SIM and RIM maximum wave height results. The lower axis shows the model and data wave heights at the Port Orford tide gauge.

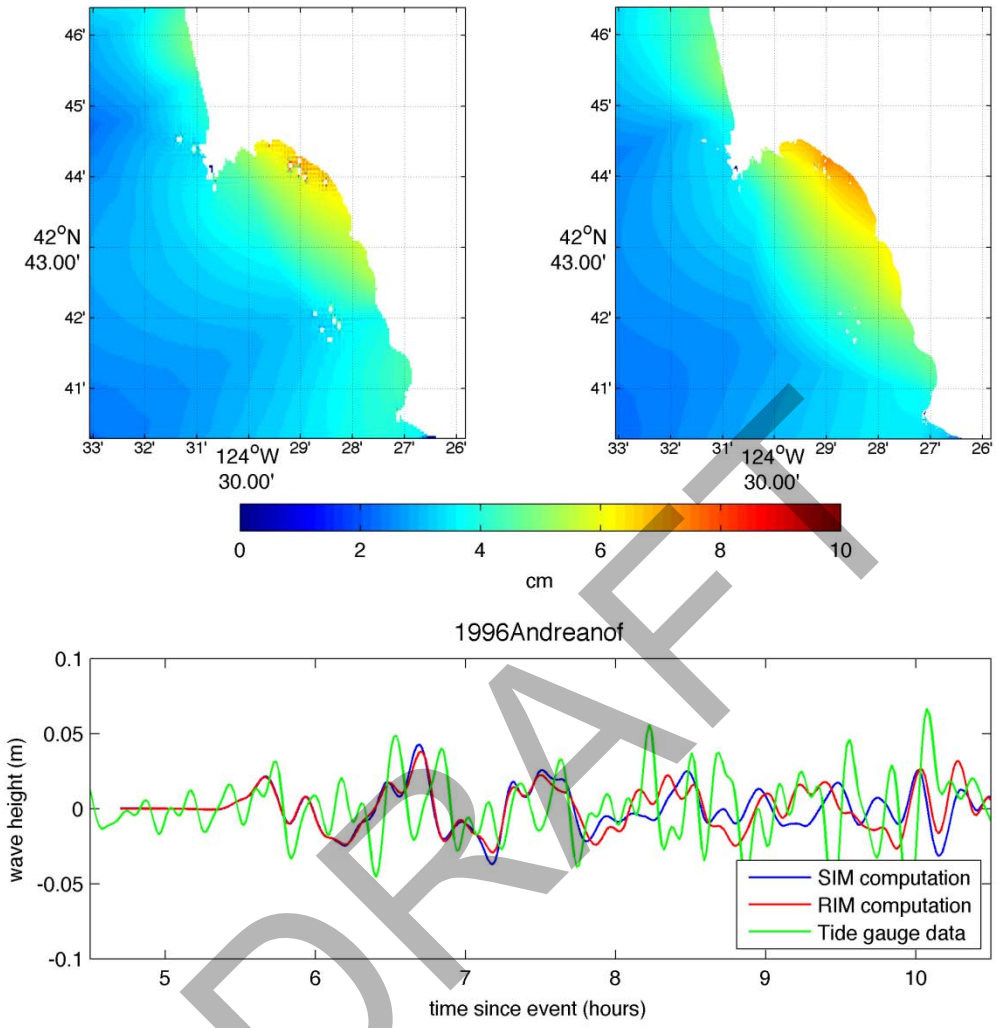

DRAFT

Figure 7 Model results for the 1996 Andreanof event. Top left and right axes show, respectively, the SIM and RIM maximum wave height results. The lower axis shows the model and data wave heights at the Port Orford tide gauge.

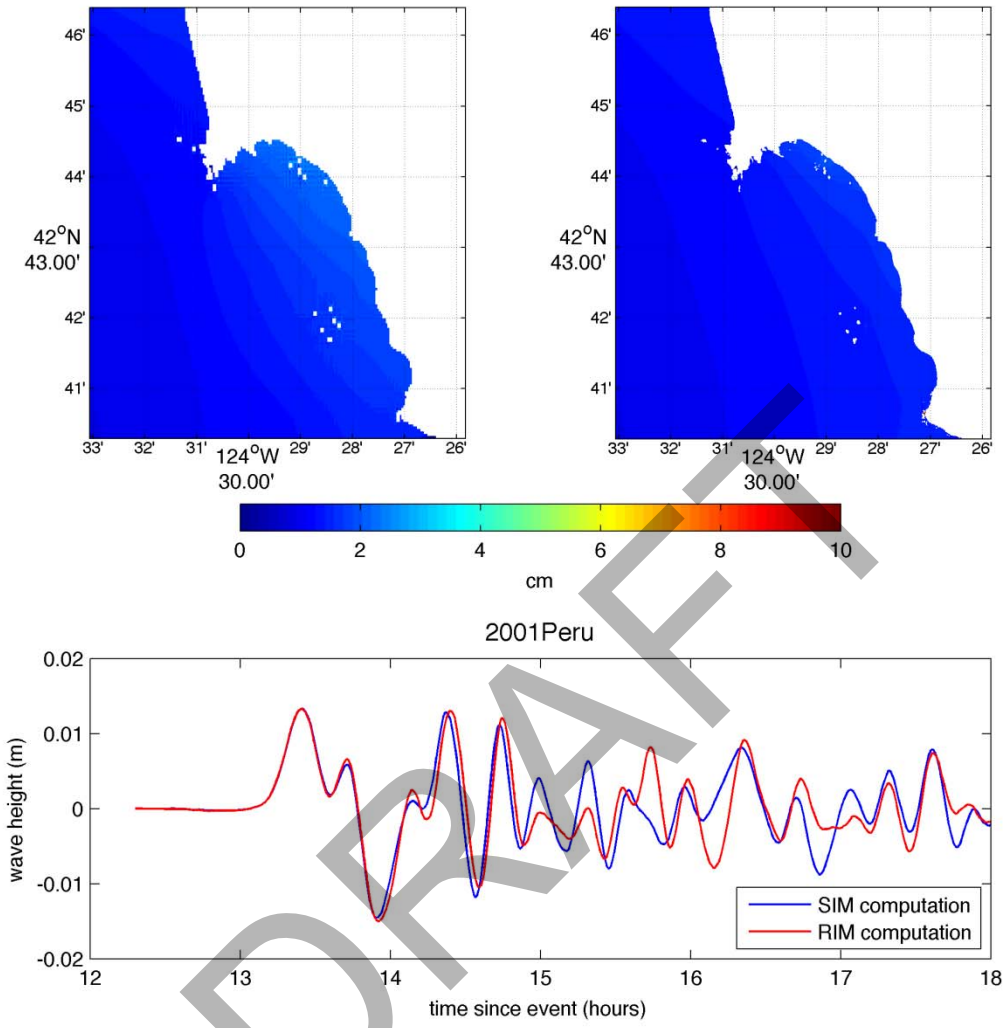

DRAFT

Figure 8 Model results for the 2001 Peru event. Top left and right axes show, respectively, the SIM and RIM maximum wave height results. The lower axis shows the model wave heights at the geographical position of the Port Orford tide gauge.

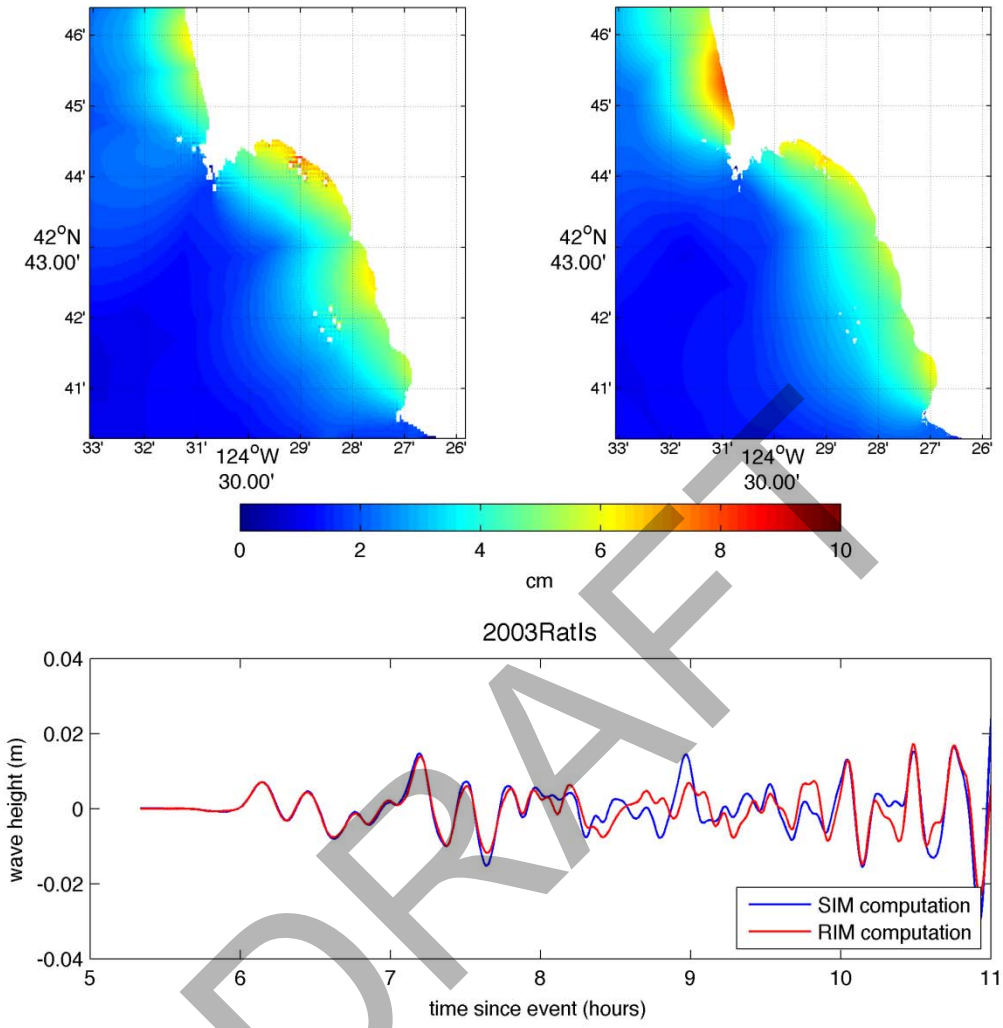

DRAFT

Figure 9 Model results for the 2003 Rat Island event. Top left and right axes show, respectively, the SIM and RIM maximum wave height results. The lower axis shows the model wave heights at the geographical position of the Port Orford tide gauge.

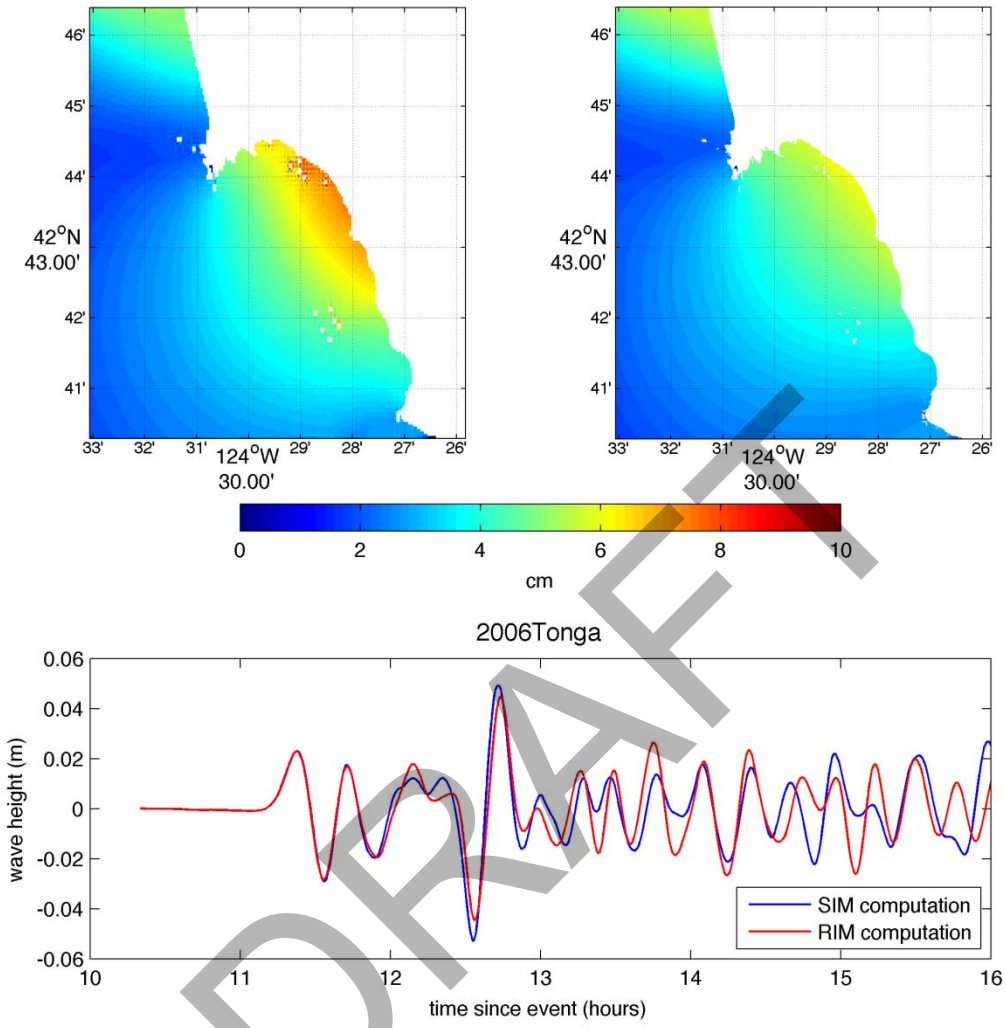

DRAFT

Figure 10 Model results for the 2006 Tonga event. Top left and right axes show, respectively, the SIM and RIM maximum wave height results. The lower axis shows the model wave heights at the geographical position of the Port Orford tide gauge.

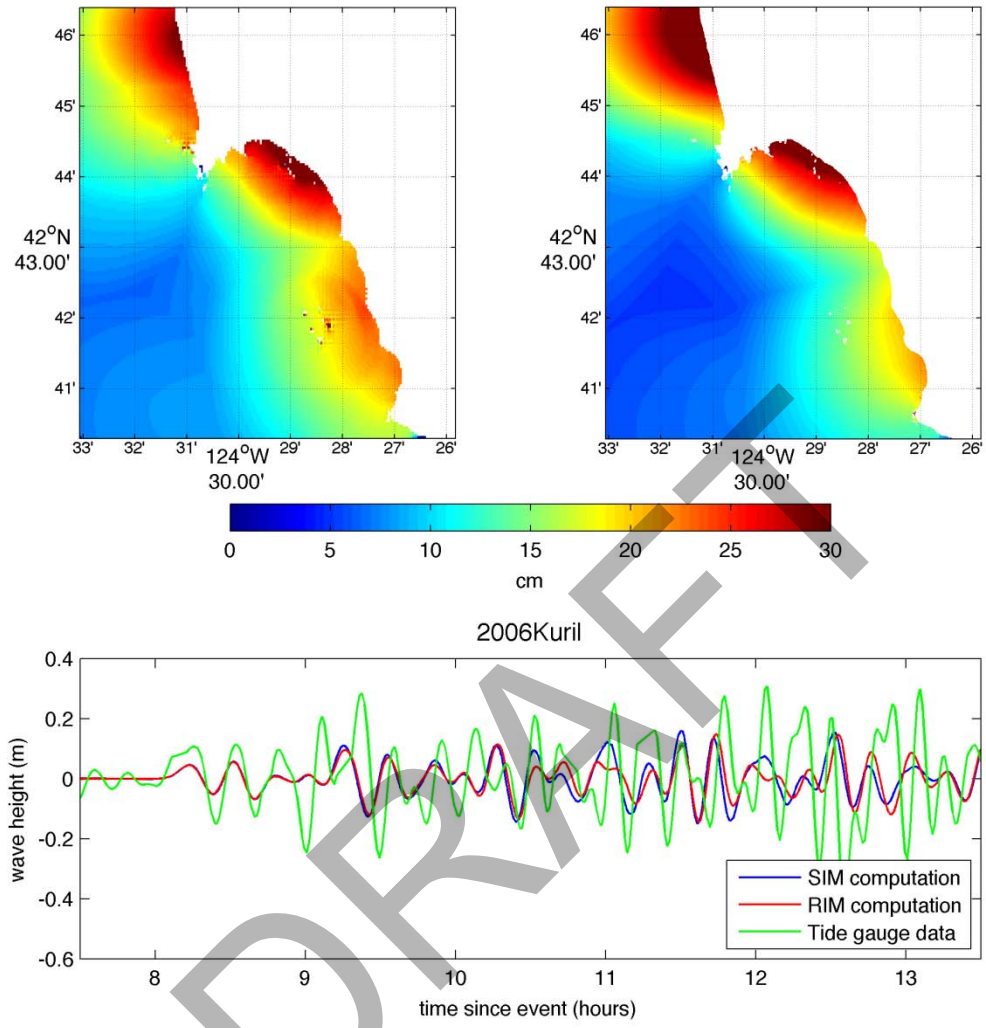

DRAFT

Figure 11 Model results for the 2006 Kuril event. Top left and right axes show, respectively, the SIM and RIM maximum wave height results. The lower axis shows the model and data wave heights at the Port Orford tide gauge.

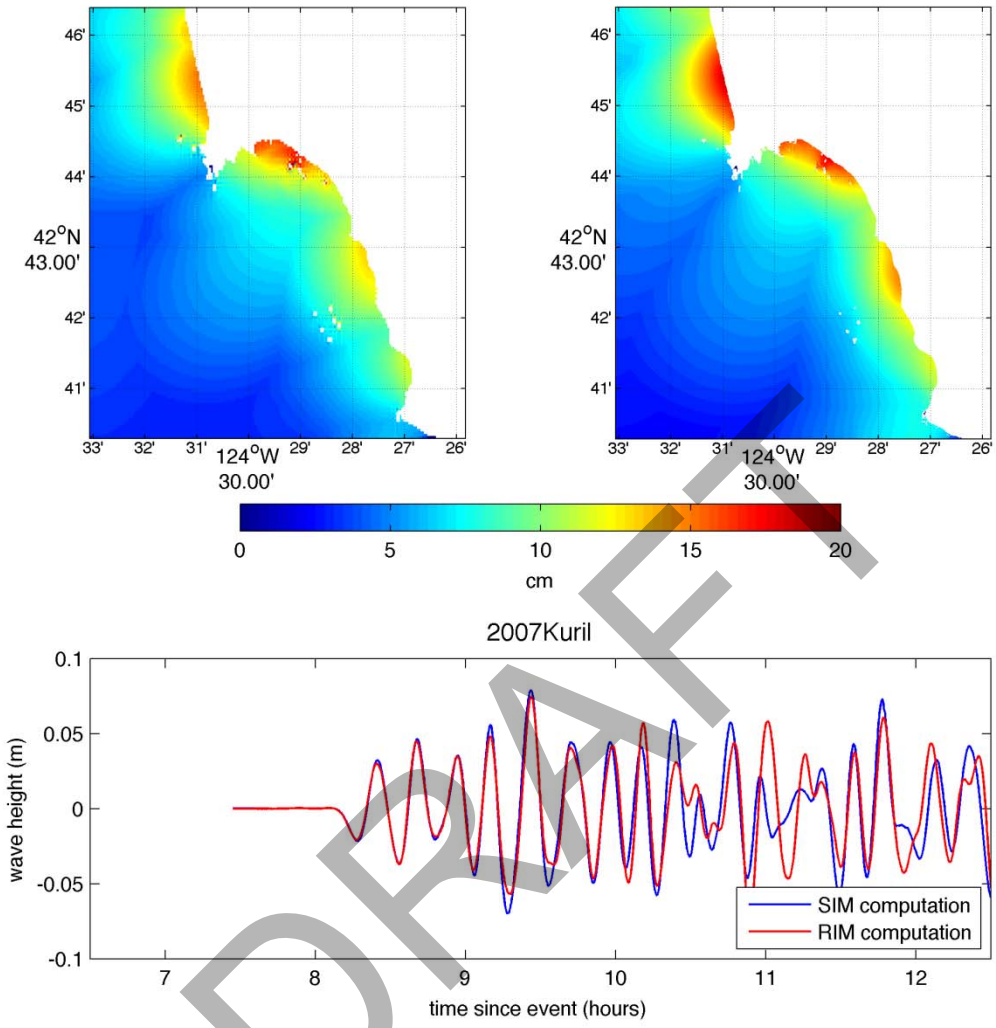

DRAFT

Figure 12 Model results for the 2007 Kuril event. Top left and right axes show, respectively, the SIM and RIM maximum wave height results. The lower axis shows the model wave heights at the geographical position of the Port Orford tide gauge.

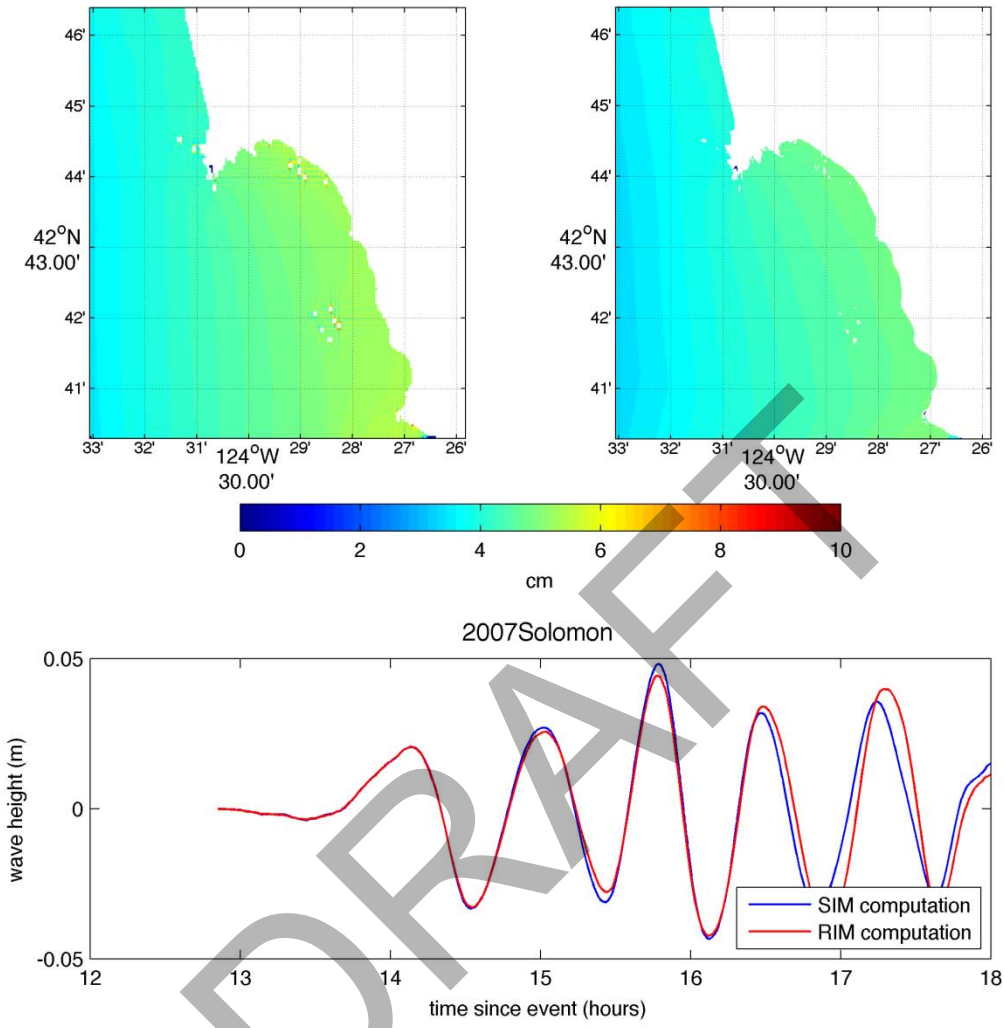

DRAFT

Figure 13 Model results for the 2007 Solomon Islands event. Top left and right axes show, respectively, the SIM and RIM maximum wave height results. The lower axis shows the model wave heights at the geographical position of the Port Orford tide gauge.

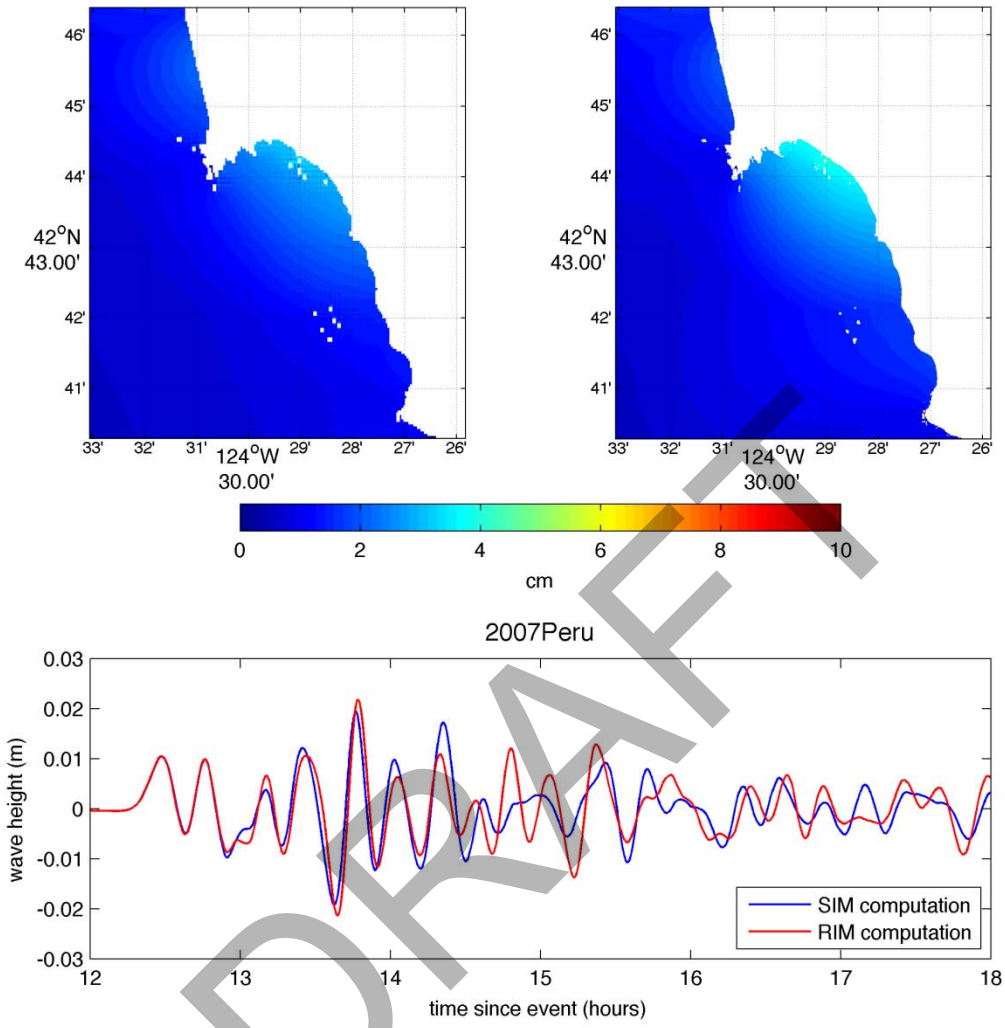

DRAFT

Figure 14 Model results for the 2007 Peru event. Top left and right axes show, respectively, the SIM and RIM maximum wave height results. The lower axis shows the model wave heights at the geographical position of the Port Orford tide gauge.

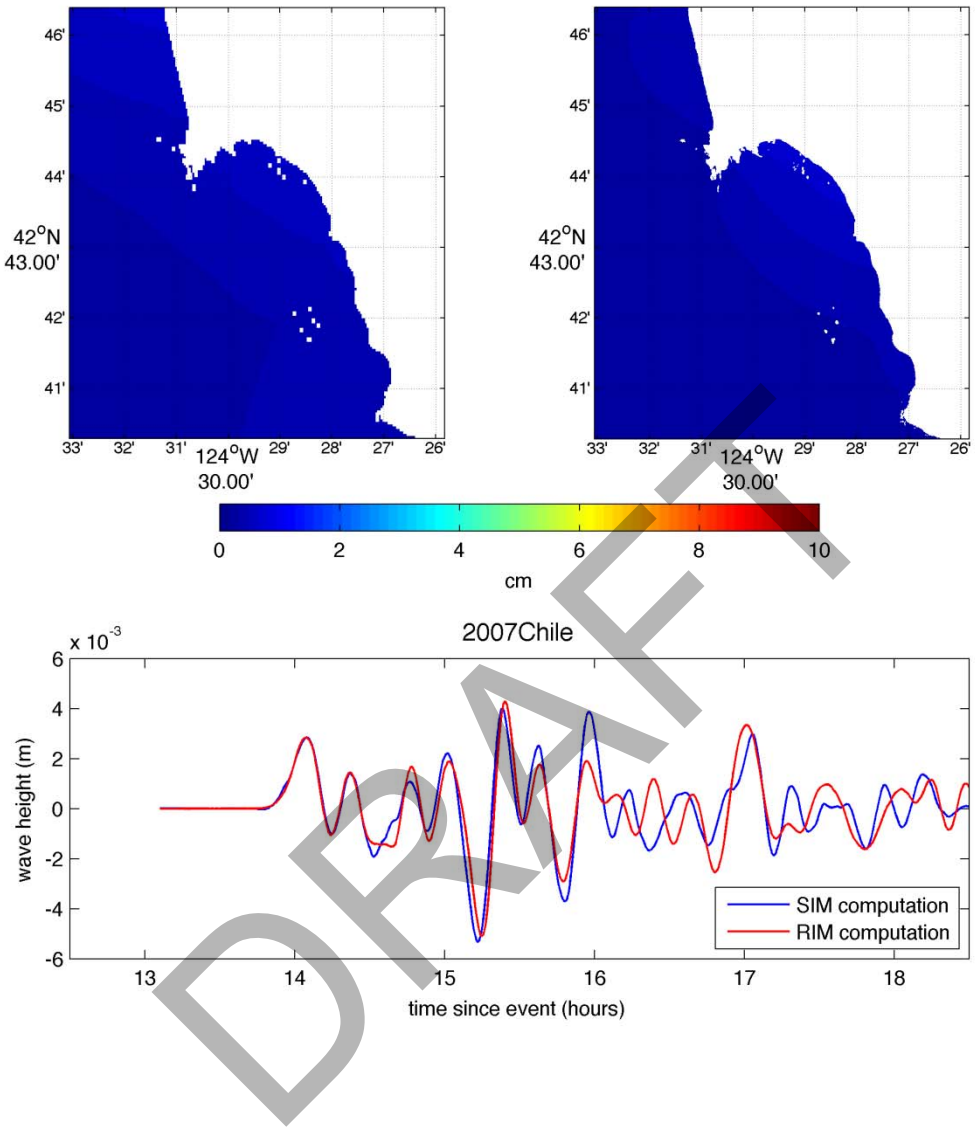

DRAFT

Figure 15 Model results for the 2007 Chile event. Top left and right axes show, respectively, the SIM and RIM maximum wave height results. The lower axis shows the model wave heights at the geographical position of the Port Orford tide gauge.

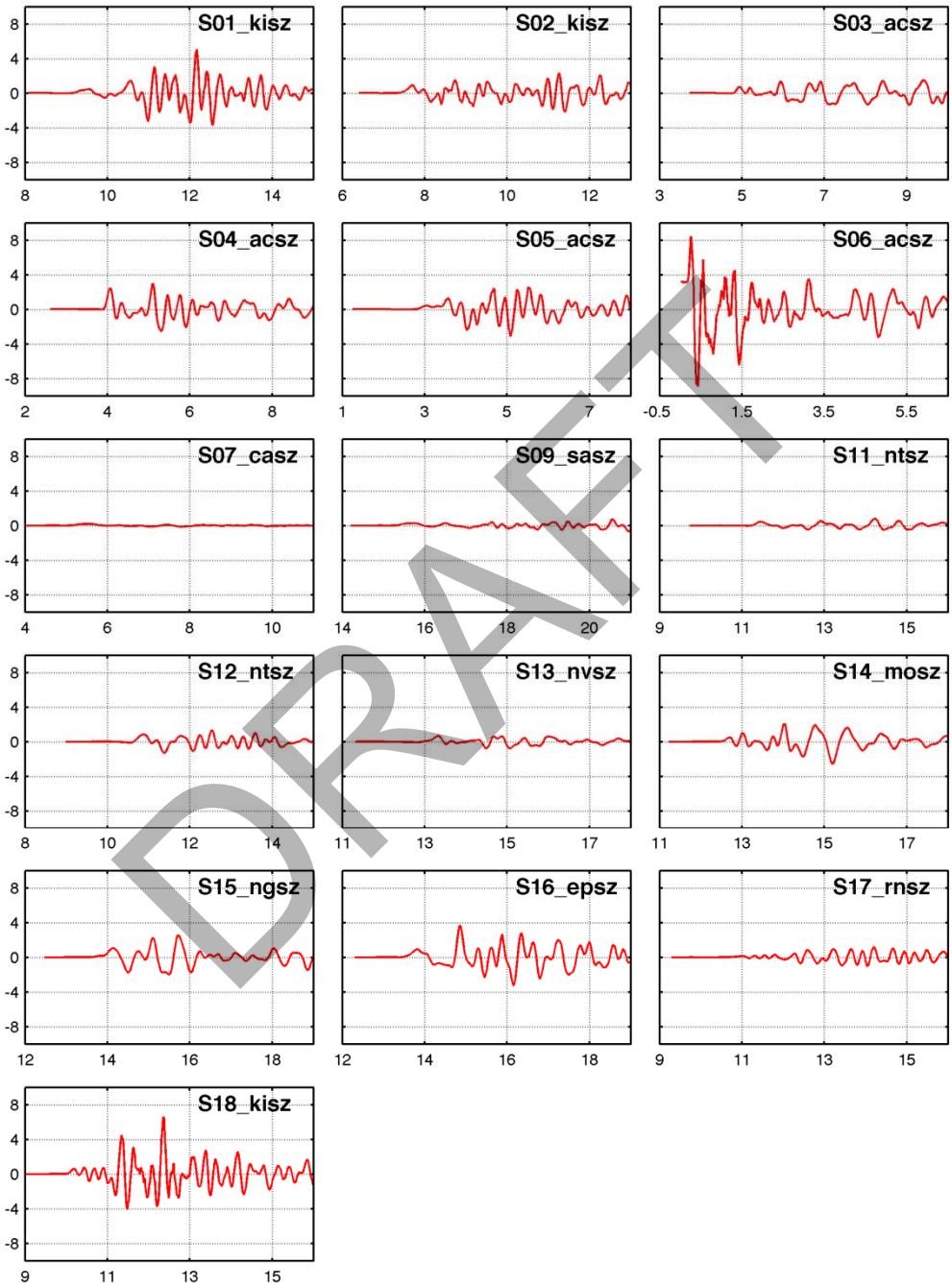

DRAFT

Figure 16 Wave heights (in meters) from the SIM model at the location of the Port Orford tide gauge for 16 hypothetical mega-tsunami scenarios. The x-axis units are hours since the event earthquake.